PULSE-WIDTH-MODULATION CONTROL OF DC-TO-DC POWER CONVERTERS: AN EXACT DISCRETIZATION APPROACH *

Maurcio García-Esteban
Instituto Tecnológico Autónomo de México
Centro de Cómputo
México, D.F., México
Phone: (525)6284000 X-1323 ; FAX: (525) 6284139
email: mauricio@itam.mx

Hebertt Sira-Ramírez
Departamento Sistemas de Control
Escuela de Ingeniería de Sistemas
Universidad de Los Andes
Mérida, Venezuela
Phone: (58)-74-442341; FAX: 58-74-402847
email isira@ing.ula.ve

June 18, 1998

Keywords: DC-to-DC Power Converters, Pulse-Width-Modulation, Exact Discretization

Abstract

In this article an exact discretization approach is developed for the Pulse-Width-Modulation (PWM) feedback control of DC-to-DC Power Converters of the "Boost" type. Contrary to existing discretization schemes, we do not rely on a state stransition matrix approach but, rather, we exploit the simplicity of the scalar differential equations representating the converter variables during the ON and OFF stages associated with the PWM regulation policy. The obtained exactly discretized linear-in-the-state and nonlinear-in-the-control first order model for the sampled values of the converter variables is used to solve a stabilization problem leading to a nonstandard regulation scheme based on an implicit feedback controller.

*This research was supported by the The Instituo Tecnológico Autónomo de Mexico (ITAM) and by the National Council for Scientific and Technological Research of Venezuela (CONICIT) under Research Grant S1-95-000886

1 Introduction

The feedback regulation of DC-to-DC power converters has been traditionally accomplished, through PWM feedback strategies (see the books by Severns, [1], Kassakian *et al*, Rashid [2] among many other authors). The control objectives typically considered include output load voltage stabilization, around a given constant value, or output voltage time-varying reference signal tracking. Such output voltage control problems are tackled in an *indirect* fashion by defining a corresponding input current stabilization or tracking problem. This procedure is justified on the basis of the non-minimum phase character of the output voltage in the "Boost", "Buck-Boost" and "Cúk" converters (The buck converter thus being atypical in this respect).

In the context of the above described problems, infinite frequency average PWM models have been frequently used at the controller design stage in order to obtain a standard nonlinear continuous-time feedback control problem resulting in a smooth state feedback specification of the conmputed duty ratio function acting as the control input. The performance of the derived feedback duty ratio control law on the actual PWM controlled circuit responses, crucially depends on the magnitude of the finite sampling frequency associated with the pulse width modulator. For relatively low sampling frequencies, the actual PWM controlled responses substantially diverge from the predicted average closed loop behaviour thus causing substantial offset errors in the stabilization and tracking tasks.

The use of average PWM models, however, may be highly questionable and not entirely justified for DC-to-DC power converters. Indeed, power supplies are constituted by picewise compositions of sufficiently simple *linear systems*, for which *exact* solutions may be readily established. Secondly, exactly discretized models, at the sampling instants, of the duty ratio - input current dynamics, or, of the duty ratio - output voltage dynamics, result, respectively, in nonlinear first order discrete-time systems for which feedback controller design methods are particularly simple.

It is the purpose of this paper to explore, in detail, the feasibility of PWM feedback controller designs for a stabilization problem defined on DC-to-DC power converter of the "boost" type. The approach is based on exact discretization of the sampled input (inductor) current rather than the output capacitor voltage, due to the non-minimum phase character of this last variable.

Discrete time regulation policies based on approximate discretization and approximate linearization were explored by Eshani *et al* in [3]. The outline of an approximate discretization approach for the stabilization of DC-to-DC power converters can also be found in Kassakian *et al* in [4]. Related developments from a viewpoint different to that of control are found in Rashid [2]. This article has been largely motivated as an extension of earlier results by the authors (see Sira-Ramírez and García-Esteban [5]) in which the simpler clase of "derived" DC-to-DC power converters are treated by similar, but considerably simpler, exact discretization methods.

The fundamental point of departure from existing discretization approaches for PWM regulated DC-to-DC power converters, is that we *do not* attempt a piecewise *state transition matrix* solution for the involved first order, linear, vector differential equations associated with each one of the switch position values taking place during a typical sampling interval of the PWM policy. The state transition matrix approach results in a surprisingly complex set of algebraic expressions that usually need questionable approximations based on series expansions, or otherwise. Our approach is based on the key observation that if the second order *scalar description* of the inductor current dynamics is exactly discretized during the "on" and the "off" stages of the commanded switch in the PWM scheme, a far simpler *first order* discrete-time model is obtained for the controlled sampled values of the inductor current. The obtained first order discrete-time model is *nonlinear* in the duty ratio, acting as the control input variable at each sampling instant, and turns out to be *linear* in the sampled values of the inductor current. Such a first order model, exactly describes the dynamics of the evenly spaced "lower peaks" of the actual zig-zagged PWM controlled inductor current trajectories. A similar first order discrete-time model can also be derived, with little additional effort, for the irregularly spaced "upper peaks" of the zig-zagged controlled inductor current trajectories. However, it turns out that the indirect output voltage steady state stabilization problem can be meaningfully solved in terms of the discretized "lower peaks" dynamical model alone, thus rendering unnecessary the consideration of the dynamical controlled behaviour of the "upper peaks".

Section 2 presents some general considerations about the exact discretization of state space models of DC-to-DC power converters and points the essential difficulties of the state transition matrix approach. Section 3 presents an alternative exact discretization approach for PWM controlled DC-to-DC converters based on the scalar input current dynamics. The obtained model is used in the definition, and solution, of the stabilization problem defined for a "boost" converter model. Section 4 is devoted to present computer simulations assessing the performance of the proposed feedback controllers for the treated converter. Section 5 contains the conclusions and suggestions for further research.

2 Generalities about Exact Discretization of PWM Controlled Converters

Traditional DC-to-DC power converters are usually modeled by first order time-invariant controlled vector differential equations of the "bi-linear" form,

$$\dot{x} = Ax + (1-u)(Bx + C) + D \tag{2.1}$$

where x is the state vector comprising inductor currents and capacitor voltages and u denotes the (single input) switch position function, taking values in the discrete set $\{0,1\}$.

A regulation strategy, based on a PWM specification of the switch position function u may be, generally speaking, specified by (see Sira-Ramírez *et al*),

$$u(t) = \begin{cases} 1 & \text{for } t_k \le t < t_k + \mu(t_k)T \\ 0 & \text{for } t_k + \mu(t_k)T \le t < t_k + T \end{cases} \tag{2.2}$$
$$t_k + 1 = t_k + T \quad \text{for } k = 0, 1, 2, \ldots$$

where $\mu(\cdot)$ is known as the *actual* duty ratio function, taking values in the closed interval $[0,1]$ of the real line. T is the sampling period (also known as the *duty cycle*) and t_k is the sampling instant. A typical example of a PWM commanded switch position function trajectory is depicted in Figure 1. For simplicity, the value of the duty ratio μ at the instant t_k will be simply denoted by μ_k instead of $\mu(t_k)$.

Since the duty ratio μ is specified online in a feedback manner, i.e., computed as a function explicitly depending on the sampled value of the state $x(t_k)$ of the converter at each instant t_k, one may obtain values of μ which lie outside the closed interval $[0,1]$. We must, therefore, make a distinction between the *computed* duty ratio function, denoted by $\mu_C(\cdot)$ and the *actual* duty ratio function, denoted by $\mu(\cdot)$. The relation between these variables is simply given by

$$\mu(t) = \begin{cases} 1 & \text{for } \mu_C(t) \ge 1 \\ \mu_C(t) & \text{for } 0 < \mu_C(t) < 1 \\ 0 & \text{for } \mu_C(t) \le 0 \end{cases} \tag{2.3}$$

The actual duty ratio function is, thus, the forceful limitation of the computed duty ratio function to the closed interval $[0,1]$.

An exact discretization of the dynamics (2.1)-(2.2) involves computation of the state vector $x(t)$ at the generic instants $t_k + \mu_k T$ and $t_k + T = t_{k+1}$. Denoting by $\Phi_A(t_1, t_2)$ and $\Phi_{A+B}(t_2, t_3)$ the state transition matrices associated with the matrices A and $A+B$ for the arbitrary time intervals (t_1, t_2) and (t_2, t_3), respectively one may obtain the following general forms of the state vector at the end of the switched pulse and at the end of the sampling interval,

$$x(t_k + \mu_k T) = \Phi_A(t_k + \mu_k T, t_k)x(t_k) + \left[\int_{t_k}^{t_k+\mu_k T} \Phi_A(t_k + \mu_k T, \sigma)d\sigma\right] D \tag{2.4}$$

$$x(t_{k+1}) = \Phi_{A+B}(t_{k+1}, t_k + \mu_k T)x(t_k + \mu_k T) + \left[\int_{t_k+\mu_k T}^{t_{k+1}} \Phi_{A+B}(t_{k+1}, \sigma)d\sigma\right](C + D) \tag{2.5}$$

An exact discretized model relating the consecutive sampled values, at times t_{k+1} and t_k, of the state vector $x(t)$, involves the elimination of the intermediate state vector value $x(t_k + \mu_k T)$, at the end of the "on" stage of the switched pulse. This yields the following general discrete-time controlled model for the sampled values of the state vector $x(t)$

$$
\begin{aligned}
x(t_{k+1}) \quad = \quad & \Big[\Phi_{A+B}(t_{k+1},t_k+\mu_k T)\Phi_A(t_k+\mu_k T,t_k)\Big]x(t_k) \\
& +\Big\{\Phi_{A+B}(t_{k+1},t_k+\mu_k T)\left[\int_{t_k}^{t_k+\mu_k T}\Phi_A(t_k+\mu_k T,\sigma)d\sigma\right]D \\
& \quad +\left[\int_{t_k+\mu_k T}^{t_{k+1}}\Phi_{A+B}(t_{k+1},\sigma)d\sigma\right](C+D)\Big\}
\end{aligned}
\tag{2.6}
$$

Similarly, if a dynamical model were needed describing the intermediate values of the states at the end of the "on" stages of the switched pulse, one could proceed to eliminate the sampled value of the state $x(t_{k+1})$ in a set of equations similar to (2.4) and (2.5). Alternatively, one could regard (2.4) as an "output" equation for the state model (2.6), eventhough its time occurence of the actual output is shifted with respect to that of the sampled state vector. i.e.,

$$
y(t_k)=[\Phi_A(t_k+\mu_k T,t_k)]\,x(t_k)+\left[\int_{t_k}^{t_k+\mu_k T}\Phi_A(t_k+\mu_k T,\sigma)d\sigma\right]D
\tag{2.7}
$$

The exactly discretized state space models (2.6) and (2.7) are, evidently, linear in the state vector components, while being highly nonlinear in the control input variable μ_k, depending on the nature of the involved state transition matrices. Unfortunately, the surprising algebraic complexity of the matrices involved in the above linear models, even for the simplest converter, render it unfeasible, and rather discouraging, any attempt to devise feedback regulation strategies based on such exactly discretized state vector models. In the following sections we propose a simpler and efficient approach for the exact discretization of the continuous time controlled models for DC-to-DC power converters .

3 An Exact Discretization of the PWM controlled Boost Converter Circuit

3.1 Description of the swtiched model

Consider the ideal boost converter circuit (see Figure 2). The mathematical state space model of such a converter is given by the following set of controlled differential equations,

$$
\begin{aligned}
\dot{x}_1 &= (1-u)\frac{1}{L}x_2+\frac{E}{L} \\
\dot{x}_2 &= -(1-u)\frac{1}{C}x_1-\frac{1}{RC}x_2 \\
y &= x_1
\end{aligned}
\tag{3.8}
$$

where u denotes the switch position function, taking values on the discrete set $\{0,1\}$. The state variable x_1 represents the (input) inductor current and x_2 represents the (output) capacitor, or load, voltage. The circuit parameters L, C and R and the external voltage source E are assumed to be known constants.

In order to simplify the notation, we use the output variable notation, y, to express the input current of the circuit, and use the variable, z, to denote the output capacitor voltage.

The linear nature of the two possible topologies of the converter circuit facilitate the derivation of an exact discrete-time model for the evolution of the sampled values of the input current, or the outupt voltage, of the boost converter (3.8) when subject to a switching policy of the form (2.2).

3.2 Scalar linear time invariant models for each switch position

Consider the case when the switch position adopts the value, $u=1$, on the interval $[t_k,t_k+\mu_k T]$; $k=0,1,2,\ldots$. In such a case, two decoupled circuits are obtained, as shown in Figure 3. The differential equations, and the associated intial conditions, describing the circuit state variables evolution, $y(t)$ and $z(t)$, are given by,

$$\begin{aligned} \dot{y}(t) &= \frac{E}{L} \ ; \ y(t_k) = y_k \\ \dot{z}(t) &= -\left(\frac{1}{RC}\right) z(t) \ ; \ z(t_k) = z_k \end{aligned} \tag{3.9}$$

whose general solutions at the instant $t = t_k + \mu_k T$, in terms of the corresponding inital values (y_k, z_k) at the sampling instant, $t = t_k$, are given by

$$\begin{aligned} y(t_k + \mu_k T) &= y_k + \frac{E}{L}\mu_k T \\ z(t_k + \mu_k T) &= \exp\left(-\frac{1}{RC}\mu_k T\right) z_k \end{aligned} \tag{3.10}$$

also, the values of the time derivatives of these state variables, at the instant $t_k + \mu_k T$, are obtained, using (3.9), as,

$$\begin{aligned} \dot{y}(t_k + \mu_k T) &= \frac{E}{L} \\ \dot{z}(t_k + \mu_k T) &= -\frac{1}{RC}\exp\left(-\frac{1}{RC}\mu_k T\right) z_k \end{aligned} \tag{3.11}$$

Consider now the case when the switch position function takes the value $u = 0$, in the time interval $[t_k + \mu_k T, t_{k+1}]$. The resulting circuit is shown in Figure 4. The differential equations describing the evolution of the state variables $y(t)$ and $z(t)$ are now given by a set of linear, time-invariant, second order, scalar differential equations,

$$\begin{aligned} \ddot{y} + \frac{1}{RC}\dot{y} + \frac{1}{LC}\left(y - \frac{E}{R}\right) &= 0 \\ \ddot{z} + \frac{1}{RC}\dot{z} + \frac{1}{LC}(z - E) &= 0 \end{aligned} \tag{3.12}$$

with initial conditions, at time $t_k + \mu_k T$, are given respectively by

$$y(t_k + \mu_k T) = y_k + \frac{E}{L}\mu_k T \ ; \ \dot{y}(t_k + \mu_k T) = \frac{E}{L} \tag{3.13}$$

$$z(t_k + \mu_k T) = \exp\left(-\frac{1}{RC}\mu_k T\right) z_k \ ; \ \dot{z}(t_k + \mu_k T) = -\frac{1}{RC}\exp\left(-\frac{1}{RC}\mu_k T\right) z_k \tag{3.14}$$

The *modes*, or eigenvalues, associated with either one of the above described differential equations (3.12), are given by the solutions of the following characteristic equation in the complex variable s,

$$s^2 + \frac{1}{RC}s + \frac{1}{LC} = 0 \tag{3.15}$$

The roots of the characteristic equation, (3.15), are given by,

$$m_1 = -\frac{1}{2RC} - \sqrt{\frac{1}{4R^2C^2} - \frac{1}{LC}} \ ; \ m_2 = -\frac{1}{2RC} + \sqrt{\frac{1}{4R^2C^2} - \frac{1}{LC}} \tag{3.16}$$

We assume, in the interest of simplicity, but also while capturing the essential characteristics of a real life converter (see Sira-Ramírez [6]), that the following relation holds valid, among the values of the circuit parameters, L, C and R,

$$\frac{L}{C} > 4R^2 \tag{3.17}$$

i.e., the roots of the algebraic equation (3.15) are both real and strictly negative with $0 > m_2 > m_1$.

3.3 A discrete time model for the sampled values of the state variables

The general solutions, at time t, of the above set of linear second order equations, in terms of initial conditions at time $t_k + \mu_k T$ are known to be given by

$$
\begin{aligned}
y(t) &= \frac{E}{R} + \frac{1}{m_2 - m_1}\Big\{ \left(m_2 e^{m_1(t-t_k-\mu_k T)} - m_1 e^{m_2(t-t_k-\mu_k T)}\right) \left[y(t_k+\mu_k T) - \frac{E}{R}\right] \\
&\quad + \left(e^{m_2(t-t_k-\mu_k T)} - e^{m_1(t-t_k-\mu_k T)}\right) \dot{y}(t_k+\mu_k T)\Big\} \\
z(t) &= E + \frac{1}{m_2 - m_1}\Big[\left(m_2 e^{m_1(t-t_k-\mu_k T)} - m_1 e^{m_2(t-t_k-\mu_k T)}\right) [z(t_k+\mu_k T) - E] + \\
&\quad \left(e^{m_2(t-t_k-\mu_k T)} - e^{m_1(t-t_k-\mu_k T)}\right) \dot{z}(t_k+\mu_k T)\Big]
\end{aligned} \tag{3.18}
$$

In particular, the corresponding values of $y(t)$ and $z(t)$ at the sampling instant t_{k+1}, can be expressed in terms of the sampled values at time t_k, with the aid of the expressions for the intial conditions (3.13) and (3.14). The exactly discretized dynamical model for the inductor current and the output voltage, at the sampling times, are given, respectively, by the following linear-in-the state, nonlinear-in-the-control, set of first order difference equations,

$$
\begin{aligned}
y_{k+1} &= \frac{1}{m_2 - m_1}\left[\left(m_2 e^{m_1(1-\mu_k)T} - m_1 e^{m_2(1-\mu_k)T}\right)\right] y_k \\
&\quad + \frac{1}{m_2 - m_1}\left[(1 - m_1\mu_k T)e^{m_2(1-\mu_k)T} - (1 - m_2\mu_k T)e^{m_1(1-\mu_k)T}\right] \frac{E}{L} \\
&\quad + \frac{1}{m_2 - m_1}\left[m_2(1 - e^{m_1(1-\mu_k)T}) - m_1(1 - e^{m_2(1-\mu_k)T})\right] \frac{E}{R}
\end{aligned} \tag{3.19}
$$

$$
\begin{aligned}
z_{k+1} &= \frac{1}{m_2 - m_1}\left[m_2 e^{m_2(1-\mu_k)T} - m_1 e^{m_1(1-\mu_k)T}\right] e^{(m_1+m_2)\mu_k T} z_k \\
&\quad + \frac{1}{m_2 - m_1}\left[m_2(1 - e^{m_1(1-\mu_k)T}) - m_1(1 - e^{m_2(1-\mu_k)T}\right] E
\end{aligned} \tag{3.20}
$$

where we have chosen to express the quantity $-1/RC$ as $m_1 + m_2$.

3.4 Steady-state considerations for the definition of a stabilization problem

We now analyze the behaviour of the steady state sampled inductor current y_k and sampled capacitor voltage z_k, on the basis of the linear time-varying first order dynamics described by (3.19) and (3.20). First, we notice that the exactly discretized models (3.19) and (3.20) are of the form

$$
\begin{aligned}
y_{k+1} &= \lambda_y(t_k, \mu_k) y_k + \rho_y(t_k, \mu_k) \\
z(k+1) &= \lambda_z(t_k, \mu_k) z_k + \rho_z(t_k, \mu_k)
\end{aligned} \tag{3.21}
$$

The time-varying, control-dependent eigenvalues, $\lambda_y(t_k, \mu_k)$ and $\lambda_z(t_k, \mu_k)$, associated with the sampled inductor current and sampled capacitor voltage dynamics (3.19),(3.20), turn out to be strictly positive, strictly less than 1, except for $\lambda_y(t_k, \mu_k)$ which is 1 when μ_k is identically 1, and given by,

$$
\begin{aligned}
\lambda_y(t_k, \mu_k) &= \frac{1}{m_2 - m_1}\left[\left(m_2 e^{m_1(1-\mu_k)T} - m_1 e^{m_2(1-\mu_k)T}\right)\right] \\
\lambda_z(t_k, \mu_k) &= \frac{1}{m_2 - m_1}\left[\left(m_2 e^{m_2(1-\mu_k)T} - m_1 e^{m_1(1-\mu_k)T}\right)\right] e^{[(m_1+m_2)\mu_k T]}
\end{aligned} \tag{3.22}
$$

The steady-state value of the sampled inductor current and of the capacitor voltage, denoted, respectively by y_∞^-, and z_∞^+ corresponding to a *constant* value of the duty ratio function, denoted by μ_∞, are then readily obtained from (3.19) and (3.20) as,

$$y_\infty^- = \frac{E}{R} + \left[\frac{(1-m_1\mu_\infty T)e^{m_2(1-\mu_\infty)T} - (1-m_2\mu_\infty T)e^{m_1(1-\mu_\infty)T}}{m_2\left(1-e^{m_1(1-\mu_\infty)T}\right) - m_1\left(1-e^{m_2(1-\mu_\infty)T}\right)}\right]\frac{E}{L} \tag{3.23}$$

$$z_\infty^+ = \left[\frac{m_2(1-e^{m_1(1-\mu_\infty)T}) - m_1(1-e^{m_2(1-\mu_\infty T)})}{m_2(1-e^{m_2(1-\mu_\infty)T}e^{(m_1+m_2)\mu_\infty T}) - m_1(1-e^{m_1(1-\mu_\infty)T}e^{(m_1+m_2)\mu_\infty T}}\right]E \tag{3.24}$$

The "minus sign" superscript labeling the steady state value of the inductor current variable y_∞ in (3.23) and the the "plus sign" superscript for the steady state capacitory voltage z_∞, in (3.24) refers, respectively, to the "lower" and "upper" corners of the actual zig-zagged trajectory described by the PWM control responses of each of the converter state variables. The choice of signs portrays the fact that the inductor current grows during the "ON" phase of the PWM strategy and decreases during the "OFF" phase producing the lowest vale at the end of the sampling interval. Conversely, the capacitor voltage decreases during the "ON" phase and actually increases the "OFF" phase of the PWM specified sequence of switch positions.

In order to determine the steady state values of the "ripple" associated with such trajectories, we determine the steady state value of the "upper" corners associated with the steady state PWM controlled inductor current trajectory as well as the "lower" corners corresponding to the PWM controlled capacitor voltage trajectory. According to (3.10) and (3.11) these are given simply by

$$\begin{aligned} y_\infty^+ &= y_\infty^- + \frac{E}{L}\mu_\infty T \\ &= \frac{m_2 - m_1}{m_2\left[1-e^{m_1(1-\mu_\infty)T}\right] - m_1\left[1-e^{m_2(1-\mu_\infty)T}\right]}\frac{E}{L}\mu_\infty T \\ &\quad + \frac{e^{m_2(1-\mu_\infty)T} - e^{m_1(1-\mu_\infty)T}}{m_2\left[1-e^{m_1(1-\mu_\infty)T}\right] - m_1\left[1-e^{m_2(1-\mu_\infty)T}\right]}\frac{E}{L} + \frac{E}{R} \end{aligned} \tag{3.25}$$

and

$$z_\infty^- = \left[\frac{m_2(1-e^{m_1(1-\mu_\infty)T}) - m_1(1-e^{m_2(1-\mu_\infty T)})}{m_2(1-e^{m_2(1-\mu_\infty)T}e^{(m_1+m_2)\mu_\infty T}) - m_1(1-e^{m_1(1-\mu_\infty)T}e^{(m_1+m_2)\mu_\infty T})}\right]e^{(m_1+m_2)\mu_\infty T}E \tag{3.26}$$

The steady state "ripples" in the inductor current and in the capacitor voltage denoted, respectively, by r_∞^y and r_∞^z, are described by the following differences,

$$\begin{aligned} r_\infty^y &= y_\infty^+ - y_\infty^- = \frac{E}{L}\mu_\infty T \\ r_\infty^z &= z_\infty^+ - z_\infty^- = E(1-e^{(m_1+m_2)\mu_\infty T})z_\infty^+ \end{aligned} \tag{3.27}$$

Evidently, one always has $y_\infty^+ > y_\infty^-$ and $z_\infty^+ > z_\infty^-$ for every constant, nonzero, steady state value of the duty ratio function. However, z_∞^+ takes place at the end of the sampling interval (i.e., end of the "OFF" stage), while y_∞^+ takes place at the end of the switched pulse (i.e., at the end of the "ON" stage), which clearly shows that the voltage and current zigzagged signals are, roughly speaking, in "counterphase" i.e., while one grows the other dicreases and viceversa.

We define the steady state average value for the output voltage trajectory as,

$$y_{av}(\infty) = y_\infty^+ + \frac{1}{2}r_\infty^y = \frac{1}{2}\left(y_\infty^- + y_\infty^+\right) \tag{3.28}$$

Similarly,

$$z_{av}(\infty) = z_\infty^+ + \frac{1}{2}r_\infty^z = \frac{1}{2}\left(z_\infty^- + z_\infty^+\right) \tag{3.29}$$

Using the expressions, (3.26) and (3.14) in (3.28) one obtains,

$$
\begin{aligned}
y_{av}(\infty) \quad &= \quad \frac{E}{R} + \frac{E}{2L}\left[\frac{2e^{m_2(1-\mu_\infty T)} - 2e^{m_1(1-\mu_\infty T)}}{m_2(1-e^{m_1(1-\mu_\infty)T}) - m_1(1-e^{m_2(1-\mu_\infty)T}}\right]E \\
&\quad + \frac{E}{2L}\left[\frac{m_2\mu_\infty T(1+e^{m_1(1-\mu_\infty)T}) - m_1\mu_\infty T(1+e^{m_2(1-\mu_\infty T)})}{m_2(1-e^{m_1(1-\mu_\infty)T}) - m_1(1-e^{m_2(1-\mu_\infty)T}}\right]E \qquad (3.30) \\
& \qquad (3.31)
\end{aligned}
$$

and, in the corresponding fashion,

$$
z_{av}(\infty) \quad = \quad \frac{E}{2}\left[\frac{m_2(1-e^{m_1(1-\mu_\infty)T}) - m_1(1-e^{m_2(1-\mu_\infty)T})}{m_2(1-e^{m_2(1-\mu_\infty)T}e^{(m_1+m_2)\mu_\infty T}) - m_1(1-e^{m_1(1-\mu_\infty)T})}\right]\left(1+e^{(m_1+m_2)\mu_\infty T}\right) \qquad (3.32)
$$

$$ (3.33) $$

In order to express the steady state value of the sampled values of the inductor current y_∞^- in terms of the desired average steady state value of the capacitor voltage $z_{av}(\infty)$, one would have to eliminate the steady state duty ratio function value μ_∞ from the equations (3.32) and (3.23). This cannot be explicitly done, but it can be certainly carried out *numerically*. That is, given a desired steady state value for the average capacitor voltage, $z_{av}(\infty)$, one can always numerically, and in an off-line fashion, compute, on the basis of (3.32) and (3.23), the corresponding desired value of the steady state sampled inductor current y_∞^-, i.e., one can numerically compute the, otherwise implicit, function, $y_\infty^-(z_{av}(\infty))$. This steady state value is taken as the control objective for the discretized dynamical model of the sampled inductor current (3.19), in which the duty ratio functin plays the role of the required feedback control input.

Figure 5 shows typical curves of $z_{av}(\infty)$ and y_∞^- versus μ_∞ and the corresponding curve y_∞^- versus $z_{av}(\infty)$ obtained from the two curves just described. As it can be seen from these figures for a given $z_{av}(\infty)$ there is a *unique* y_∞^- which will serve as a constant reference value for the inductor current controlled dynamics in the indirect output voltage feedback stabilization problem.

3.5 Feedback controller design for indirect stabilization of the output voltage

In the previous section we have seen that given a desired value of the steady state average capacitor voltage, the procedure described above allows the computation of a unique corresponding value of the steady state sampled inductor current to which the trajectories of the first order discrete model (3.19) should be stabilized by means of an appropriate feedback controller, $\mu(t_k, y_k, y_\infty^-(z_{av}(\infty)))$.

A feedback controller achieveing the stabilization of the sampled inductor current y_k around the desired steady state equilibrium value y_∞^- is obtained by imposing on the discretized dynamics (3.19) the following linear asymptotically stable dynamics

$$ y_{k+1} = y_\infty^- + \alpha\ \left(y_k - y_\infty^-\right) \qquad (3.34) $$

where α is a design constant satisfying $|\alpha| < 1$, and representing the closed loop constant eigenvalue for the regulated linear tracking error inductor current dynamics (3.34). The corresponding relation to be satisfied by the feeddback control input $\mu_k$is readily obtained by comparing (3.34) with (3.19)

$$ y_\infty^- + \alpha\ \left(y_k - y_\infty^-\right) = \lambda_y(t_k, \mu_k)y_k + \rho_y(t_k, \mu_k) \qquad (3.35) $$

which leads to the relation

$$ (1-\alpha)y_\infty^- = \left[\alpha + \lambda_y(t_k, \mu_k)\right]y_k + \rho_y(t_k, \mu_k) \qquad (3.36) $$

The relation (3.18) represents an *implicit* feedback controller which yields, for a given value of the inductor current variable y_k, ocurring at the sampling instant t_k, a corresponding value of the required control input duty ratio μ_k. The numerical *on line* solution of the transcendental equation (3.18) can be greately facilitated by constructing a *table* of values of μ_k versus the actual measured inductor current y_k, for the fixed value of the desired steady state inductor current y_∞^-, off line computed on the basis of the desired average steady state capacitor voltage $z_{av}(\infty)$. Figure 6 shows the off-line as well the on-line calculations needed in the linearizing feedback control scheme yielding the required output stabilization.

References

[1] R. P. Severns and G. E. Bloom, *Modern DC-to-DC Switchmode Power Converter Circuits*, New York: Van Nostrand Rehinhold, 1983.

[2] M. Rashid, *Power Electronics, Circuits, Devices and Applications* London: Prentice Hall International, 1993.

[3] M. Ehsani, R. Kustom and R. Fuja, "Microprocessor control of a current source DC-to-DC converter" *IEEE Transactions on Industry Applications* Vol. 19, pp. 690-698, 1983.

[4] J. G. Kassakian, M. Schlecht and G. Verghese, *Principles of Power Electronics*, Reading, Massachusetts: Addison-Wesley, 1991.

[5] H. Sira-Ramírez, M. García-Esteban and R. Pérez-Moreno, "Design of pulse width modulation controllers for stabilization and tracking in derived DC-to-DC power converters" *International Journal of Control*, Vol. 64, No. 2, pp. 301-318, 1996.

[6] H. Sira-Ramírez, " Sliding Mode Control on Slow Manifolds of DC-to-DC Power Converters," *International Journal of Control*, Vol. 47, No. 5, pp. 1323-1340. Mayo 1988.

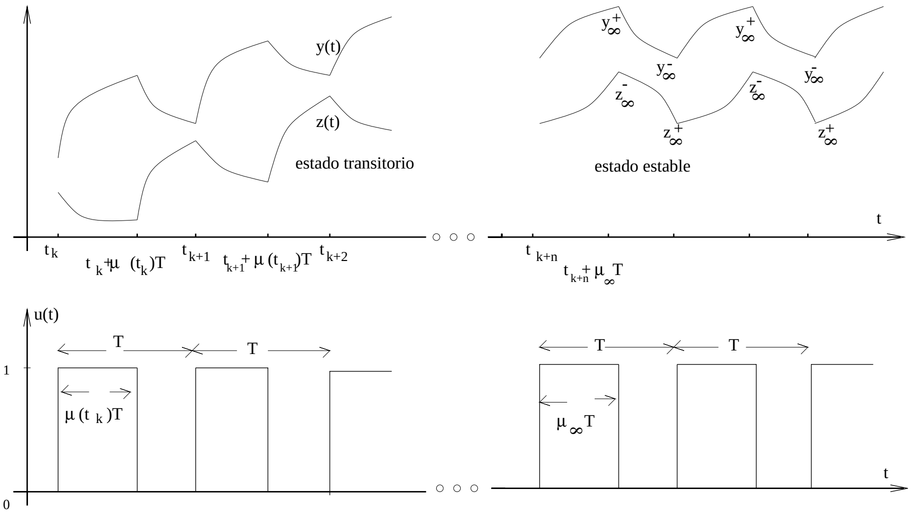

Figure 1: A typical sequence of a PWM switch position function

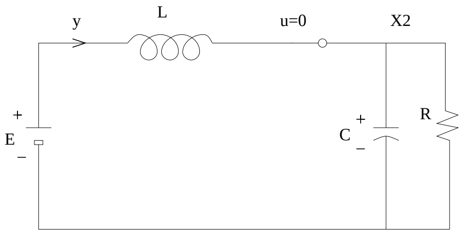

Figure 2: Boost converter circuit with switch position $u = 0$

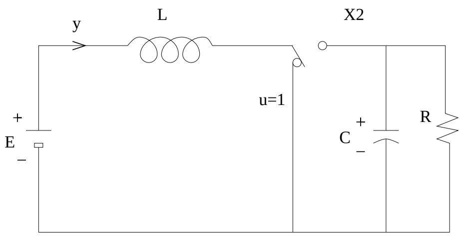

Figure 3: Boost converter circuit with switch position $u = 1$

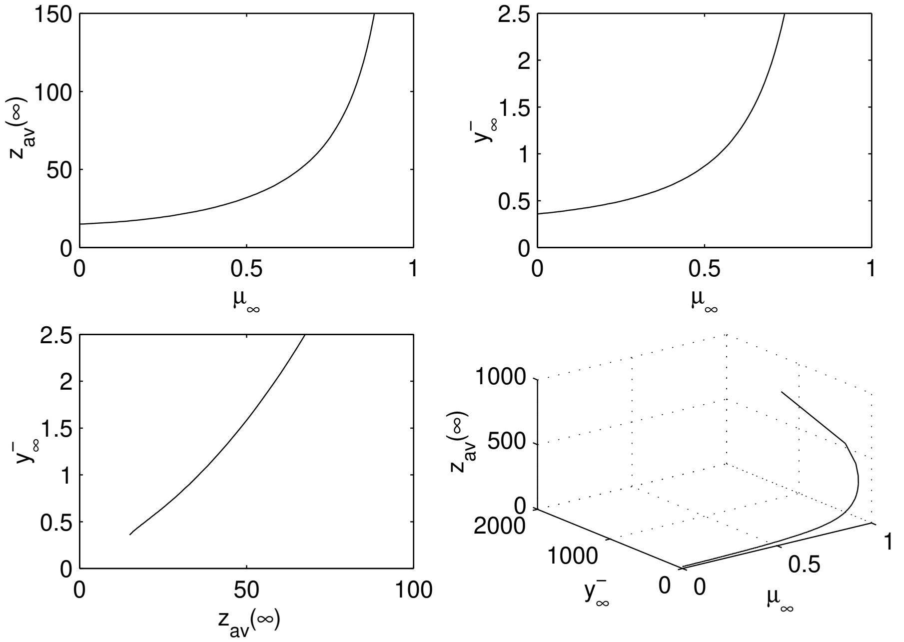

Figure 4: Determination of steady state sampled inductor current as a function of steady state average capacitor voltage

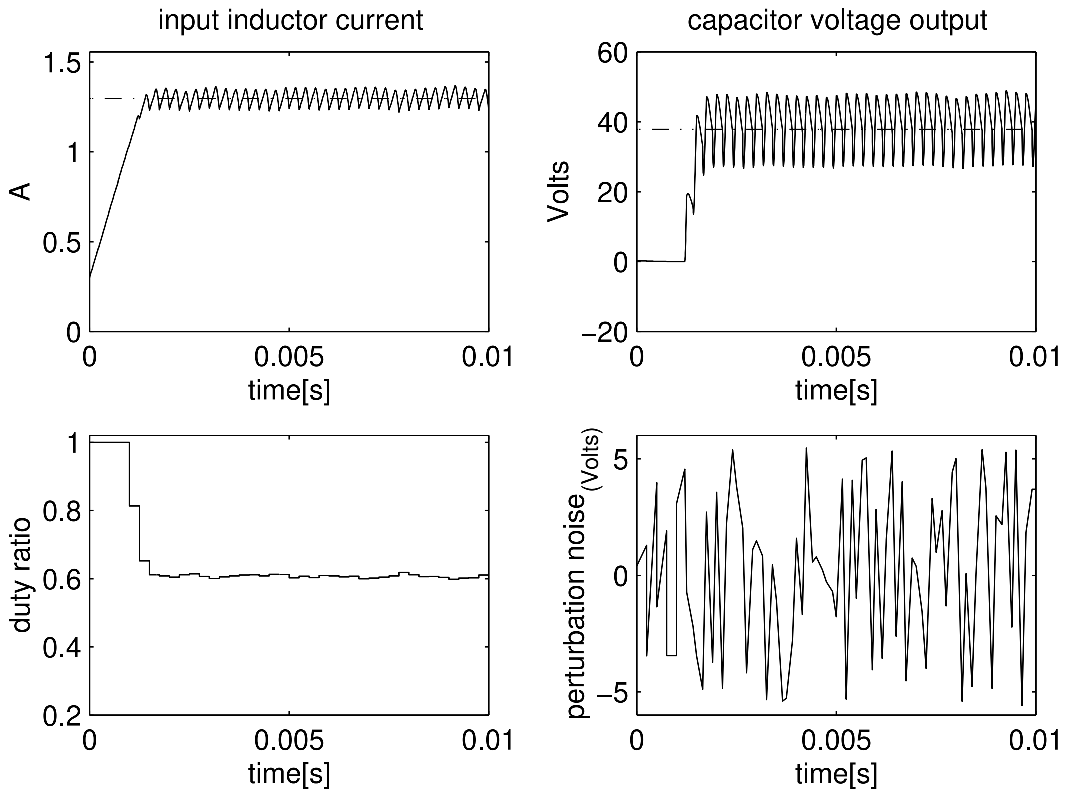

Figure 5: Simulation Results for Evaluation of the Indirect Controller in a Perturbed “boost” Converter